Appl. Phys. B 51, 132–136 (1990)

Applied Physics B Photophysics and Laser Chemistry

Temperature Dependence of the Lifetime of Cr^{3+} Luminescence in Garnet Crystals

II. The Case of YGG

M. Yamaga*, B. Henderson, K. P. O'Donnell, and G. Yue

Department of Physics and Applied Physics, University of Strathclyde, Glasgow G4 0NG, U.K.

Received 5 December 1989/Accepted 19 January 1990

Abstract. The coexistence of sharp R-lines from the ^2E state and the broad band from the $^4T_2$ state in the photoluminescence spectra of $Cr^{3+}:Gd_3Sc_2Ga_3O_{12}$ (GSGG) and $Cr^{3+}:Y_3Ga_5O_{12}$ (YGG) is observed at low temperature (10 K). The decay lifetimes of the broad emission bands of Cr^{3+} in GSGG and YGG are very close to those of the R-lines being, respectively, 0.23 ms and 2.5 ms. These results are explained in terms of the extent of the mixing of the $^4T_2$ vibronic wavefunction with that of the ^2E lowest excited state by tunnelling.

PACS: 42.70, 79.60

Chromium-doped garnets are the gain media of tunable solid-state lasers operating in the red or infrared spectral regions [1–3]. The broad band emission on which laser action is based arises from transitions out of the $^4T_2$ excited state into the $^4A_2$ ground state of Cr^{3+} ions. In contrast, the R-line and its phonon side band are due to ^2E to $^4A_2$ transitions. Whether ^2E or $^4T_2$ is the lowest excited state is determined by the strength of the octahedral crystal field surrounding Cr^{3+} ions. Cr^{3+} in $Gd_3Sc_2Ga_3O_{12}$ (GSGG) occupies intermediate crystal field sites where the $^4T_2$ and ^2E levels are very close together in energy [4–6]. The two states, when represented by vibronic wavefunctions, are separated by a potential barrier, the height of which varies with the strength of the crystal field. If the barrier is lowered until it becomes comparable with the phonon energy, tunnelling occurs between the two states and mixing of the vibronic wavefunctions results. The mixing influences the lineshapes and lifetimes of the emission from the lowest excited state of Cr^{3+} ions. In previous papers, the temperature dependence of the intensity and lifetime of the fluorescence from Cr^{3+} in various garnet crystals was explained using a tunnelling model [7, 8]. This paper discusses the lifetimes of Cr^{3+}:GSGG and $Cr^{3+}:Y_3Ga_5O_{12}$ (YGG) observed at low temperature (10 K) in terms of the theoretical values derived from the tunnelling model.

1. Experimental Procedure

Cr^{3+}-doped YGG thin films were rf-sputtered onto $Y_3Al_5O_{12}$ (YAG) substrates which had been cut and polished on the (111) plane [9]. The target was made by sintering a stoichiometric mixture of $Y_2O_3:Ga_2O_3 = 3:5$ with 1 mol% Cr_2O_3 relative to Ga_2O_3. Amorphous films grown on subtrates held at a temperature of 450°C were recrystallized by annealing in pure oxygen at 1000°C [10]. The composition of the crystalline film was estimated to be $Y_3Ga_5O_{12}$ within an experimental error (±5%) using energy dispersed X-ray spectra detected with an X-ray micro-analyser. The decay time of the fluorescence emitted by Cr^{3+} ions in YGG crystalline thin films was detected through a 1 m grating monochromator using a GaAs photomultiplier tube, a current amplifier and boxcar averager (Stanford Research Systems SR265). The excitation beam was the mechanically chopped radiation emitted at 488 nm from a 6 W Ar^+ ion laser.

* Permanent address: Department of Physics, Faculty of General Education, Gifu University, Gifu, 501-11, Japan

2. Experimental Results

Figure 1a shows the emission spectrum of Cr^{3+} in YGG at 10 K, composed of the sharp R_1-line, its phonon side band and the very weak broad band with the peak wavelength of 730 nm. The intensity of the broad band relative to that of the R-line and its phonon side band is 0.4 : 1. This ratio is calculated to be 10^{-28} assuming a Boltzman distribution between ^2E and $^4T_2$ states separated in energy by 450 cm^{-1} at 10 K [8]. Furthermore, the lifetime of the R-line from a pure ^2E state should be 100 times longer than that of the broad band from a pure $^4T_2$ state. This large discrepancy was explained by tunnelling between ^2E and $^4T_2$ levels [8]. Figure 1b shows the emission spectrum in the range 688.0–692.5 nm. The spectra are decomposed into three Gaussians with the peak wavelengths of 689.8, 690.2, and 691.5 nm. From a line-shape analysis of the R-lines of Cr^{3+} ions in mixed garnet crystals $Y_{3.1}Ga_{4.9}O_{12}$ and $Y_{3.8}Ga_{4.2}O_{12}$, the R_1-line at 689.8 nm was assigned to be a Cr^{3+} ion in stoichiometric composition $Y_3Ga_5O_{12}$, having Ga^{3+} ions in the eight nearest-neighbor octahedral sites [9]. Replacement of Ga^{3+} ions by the larger Y^{3+} ions in the octahedral sites reduces the crystal field surrounding the Cr^{3+} ions giving rise to a shift of the peak to longer wavelength. The line at 690.2 nm was assigned to the R_1-line from Cr^{3+} ions located at octahedral sites in which one of the Ga^{3+} ions occupying nearest-neighbour octahedral sites was replaced by a Y^{3+} ion [9]. Next, we consider the origin of the line at 691.5 nm.

Figure 2 shows the fluorescence decay of these lines at 10 K. The decay curve of the line at 689.8 nm is almost exponential and the lifetime is estimated to be 2.4 ms. The decay curve at 690.6 nm is not a single exponential: it may be decomposed into two components of 1.7 ms and 2.4 ms; the fast component may be associated with the Cr^{3+} sites having the weak crystal field. The decay curve at 691.5 nm is also non-exponential, and similar to that at 690.6 nm. The R-lines in garnet crystals are observed to be red-shifted with decreasing crystal field, resulting in a shortening of the lifetime [8]. The energy separation between the 689.8 nm and 691.5 nm lines is about 37 cm^{-1}. A component red-shifted by 40 cm^{-1} from the R_1-line has also been observed in Cr^{3+} : YAG [11]. If the line at 691.5 nm is an R_1-line, the lifetime should be shorter than that (2.4 ms) at 689.8 nm. However, the observed lifetime of the dominant component at 691.5 nm is similar to that at 689.8 nm. Therefore, the line at 691.5 nm is not an R_1-line from a Cr^{3+} ion in a different site, but may be the one-phonon line of the 689.8 nm line with a phonon energy of 37 cm^{-1}.

The fluorescence decays of the broad band at 760 nm and 780 nm are shown in Fig. 3 to be multi-

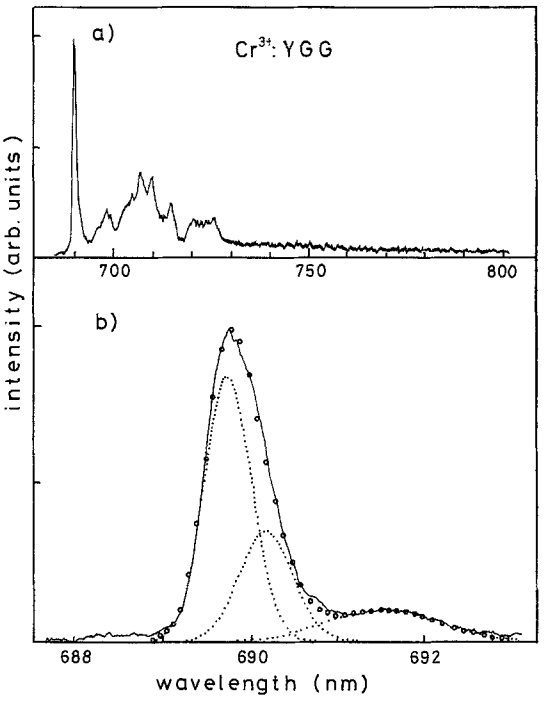

Fig. 1. **a** Fluorescence spectrum in Cr^{3+} : YGG thin film at 10 K under cw excitation with Ar^+ ion laser radiation at 488 nm. **b** The lineshape analysis of the R_1 emission lines in Cr^{3+} : YGG thin film at 10 K. The dotted lines represent decomposition into gaussian lineshapes. Open circles are the sum of the gaussian lines

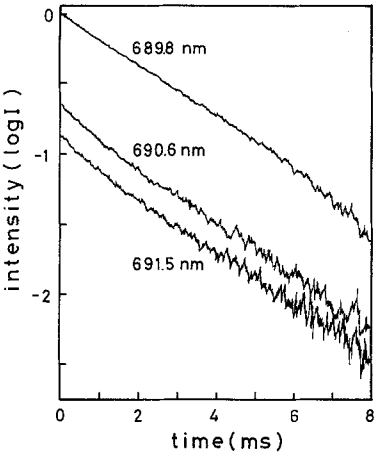

Fig. 2. Fluorescence decay curves of the emission lines at 689.8 nm, 690.6 nm, and 691.5 nm in Cr^{3+} : YGG thin film at 10 K. The emission intensities are normalized to that of the 689.8 nm component at $t = 0$ ms

exponential curves which may be decomposed into two components. The lifetimes of the slower decay component, 2.5 ms at 760 nm and 780 nm, are very close to that of R_1-line at 689.8 nm, while the lifetimes of the fast components are 0.16 ms. The time-integrated intensity ratios of the component with lifetime 0.16 ms to that with 2.5 ms at 760 nm and

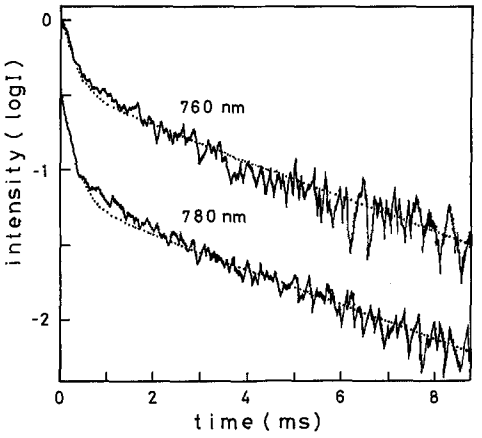

Fig. 3. Fluorescence decay curves of the broad band at 760 nm and 780 nm. The emission intensity at 760 nm is normalized to that at $t=0$ ms. The origin of the emission intensity at 780 nm is slightly shifted. The dotted lines at 760 nm and 780 nm are calculated for the radiative decay with two components of lifetimes 0.16 ms and 2.5 ms with initial intensity ratios ($t=0$ ms) 2:1 and 4:1, respectively

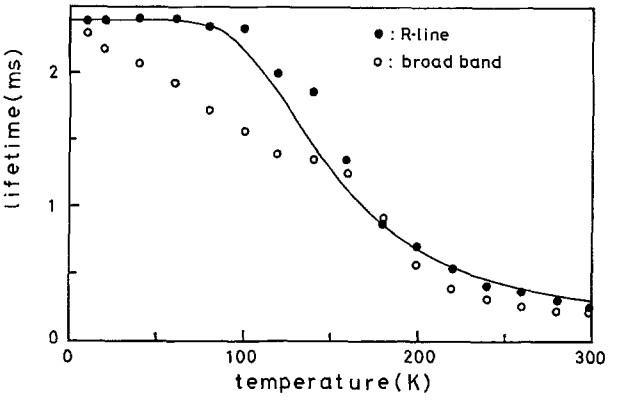

Fig. 4. Temperature dependence of the lifetimes of the R_1-line (689.8 nm) and the broad band (760 nm). The solid curve is calculated using (6) with $\tau_1=2.4$ ms, $\tau_2=40\,\mu$s, and $\Delta E=450\,\text{cm}^{-1}$

780 nm, represented by the product of the initial intensity at $t=0$ and the lifetime, are estimated to be 0.13:1 and 0.26:1, respectively, the slower component being dominant. The origin of the two components is discussed later.

Figure 4 shows the temperature dependence of the lifetimes of the R_1-line (689.8 nm) and the broad band (760 nm). The data of the broad band are the dominant component, i.e., the slower lifetime.

3. Discussion

3.1. Mixing of ^2E and $^4T_2$ States by Tunnelling

As the barrier separating the two states ^2E and $^4T_2$ is lowered until it becomes comparable with the phonon energy, the adiabatic approximation becomes invalid and tunnelling occurs between two potential minima. The wavefunctions mixed by tunnelling are given by [7, 8],

$$\begin{aligned}\Psi'_E(r,R)&=\alpha\Psi_E(r,R)+\beta\Psi_T(r,R),\\ \Psi'_T(r,R)&=\beta\Psi_E(r,R)-\alpha\Psi_T(r,R),\end{aligned}\tag{1}$$

where $\Psi_E(r,R)$ and $\Psi_T(r,R)$ are the pure vibronic wavefunctions of ^2E and $^4T_2$ states without tunnelling, and α and β are mixing coefficients which are determined by the energy separation between the ^2E and $^4T_2$ states and the tunnelling splitting [8]. The transition probabilities from levels 1 and 2 corresponding to the wavefunctions $\Psi'_E(r,R)$ and $\Psi'_T(r,R)$, and which are equal to the inverse of the lifetimes, are given under the assumption that $\Psi_E(r,R)$ is orthogonalized to $\Psi_T(r,R)$, by [8],

$$\begin{aligned}\frac{1}{\tau_1}&=\frac{\alpha^2}{\tau_E}+\frac{\beta^2}{\tau_T}\\ \frac{1}{\tau_2}&=\frac{\beta^2}{\tau_E}+\frac{\alpha^2}{\tau_T}\end{aligned}\tag{2}$$

where τ_E and τ_T are the lifetimes of the pure vibronic states $\Psi_E(r,R)$ and $\Psi_T(r,R)$.

3.2. Radiative Decay Rate

The radiative decay rates from levels 1 and 2 are calculated using the rate equation of the population on levels 1 and 2. The change of the population of levels 1 and 2, n_1 and n_2, is described by the rate equations,

$$\begin{aligned}\frac{dn_1}{dt}&=k_1-\frac{n_1}{\tau_1}-W_{12}n_1+W_{21}n_2,\\ \frac{dn_2}{dt}&=k_2-\frac{n_2}{\tau_2}-W_{21}n_2+W_{12}n_1,\end{aligned}\tag{3}$$

where k_1 and k_2 are the generation rates, W_{12} is the transition probability from level 1 to level 2. With the assumption that the radiative decay rates $(1/\tau_1, 1/\tau_2)$ are much smaller than the lattice relaxation rates (W_{12}, W_{21}), the populations of levels 1 and 2 are described by a Boltzman distribution, i.e.,

$$\frac{n_2}{n_1}=\frac{W_{12}}{W_{21}}=\exp\left(-\frac{\Delta E}{kT}\right),\tag{4}$$

where ΔE is the energy separation of ^2E and $^4T_2$.

Consider the radiative decay after excitation is switched off (i.e. $k_1=k_2=0$). The emission spectrum from level 1, i.e., the R-line and its phonon side band and the broad band, is the same as that from level 2 except that the intensity ratio from level 1 or level 2 is $(\alpha^2/\tau_E:\beta^2/\tau_T)$ or $(\beta^2/\tau_E:\alpha^2/\tau_T)$, respectively. That is, both levels 1 and 2 contribute to the R-line and the

broad band. Therefore, the change of population is rewritten in the form

$$\frac{d(n_1+n_2)}{dt} = -\frac{n_1}{\tau_1} - \frac{n_2}{\tau_2} = -\frac{n_1+n_2}{\tau}, \quad (5)$$

where

$$\frac{1}{\tau} = \frac{\frac{1}{\tau_1} + \frac{1}{\tau_2}\exp\left(-\frac{\Delta E}{kT}\right)}{1+\exp\left(-\frac{\Delta E}{kT}\right)}. \quad (6)$$

The total population, (n_1+n_2), is then given by

$$n_1+n_2 = n_0 \exp\left(-\frac{t}{\tau}\right). \quad (7)$$

The intensities of the R-line and its phonon side band and the broad band are represented by the sum of the contributions from levels 1 and 2 and given in the form

$$I_E = \alpha^2 \frac{n_1}{\tau_E} + \beta^2 \frac{n_2}{\tau_E}$$
$$I_T = \beta^2 \frac{n_1}{\tau_T} + \alpha^2 \frac{n_2}{\tau_T}. \quad (8)$$

which when rewritten using (4), (6), and (7) become:

$$I_E = \left(\frac{n_0}{\tau_E}\right)\frac{\alpha^2+\beta^2\exp\left(-\frac{\Delta E}{kT}\right)}{1+\exp\left(-\frac{\Delta E}{kT}\right)}\exp\left(-\frac{t}{\tau}\right)$$
$$I_T = \left(\frac{n_0}{\tau_T}\right)\frac{\beta^2+\alpha^2\exp\left(-\frac{\Delta E}{kT}\right)}{1+\exp\left(-\frac{\Delta E}{kT}\right)}\exp\left(-\frac{t}{\tau}\right). \quad (9)$$

Equation (9) shows that the relative intensity ratio, I_T/I_E, is given by $[\beta^2+\alpha^2\exp(-\Delta E/kT)]/[\alpha^2+\beta^2\exp(-\Delta E/kT)]$ [7, 8] and the radiative decay rates of the R-line and the broad band are the same and are given in (6).

3.3. Comparison of the Experimental Result with the Theory

The temperature dependences of the Cr^{3+} fluorescence lifetimes of Cr^{3+} ions in alexandrite [12], emerald [13], $Gd_3Ga_5O_{12}$ (GGG) [14], $Gd_3Sc_2Al_3O_{12}$ (GSAG) [15], and GSGG [5, 8, 14, 15] have been reported. The data for alexandrite, emerald, and GGG were fitted to equations calculated for a two-level system involving ^2E and $^4T_2$ levels where non-radiative decay is neglected. The appropriate equation used in Refs. [13, 14] is the same as (6) with the assumption that $\alpha^2=1$ and $\beta^2=0$. The data for Cr^{3+}:GSGG cannot be explained using this form of the equation with the observed lifetimes of 260 μs for the R-line and 230 μs for the broad band [14]. The present authors have explained the results for Cr^{3+}:GSGG using a tunnelling model [8]. The data were fitted to theory using (2) and (6) with $\tau_1=260\,\mu s$, $\tau_2=110\,\mu s$, and $\Delta E=93\,cm^{-1}$. The mixing parameters in (2) were estimated to be $\alpha^2=0.7$, $\beta^2=0.3$, $\tau_T=60\,\mu s$, and $\tau_E=4\,ms$.

The lifetime of the broad band of Cr^{3+} observed in YGG at 10 K consists of two components of 0.16 ms and 2.5 ms. First, we consider the lifetime of the dominant component (2.5 ms) using the tunnelling model. It is very close to that of the R-line (2.4 ms), and a factor of ten longer than that for Cr^{3+}:GSGG. According to the tunnelling model, the lifetime of the broad band at low temperature should be the same as that of the R-line. The lifetime given in (2) involves the mixing parameters, (α, β) and lifetimes (τ_E, τ_T). The lifetimes τ_E and τ_T for pure ^2E and $^4T_2$ states are calculated to be $\tau_E=4\,ms$ and $\tau_T=60\,\mu s$ for Cr^{3+}:YGG using the observed lifetime $\tau_1=2.4\,ms$ and mixing parameters ($\alpha^2=0.99$ and $\beta^2=0.01$) estimated from the temperature dependence of the intensity ratio, I_T/I_E, [8]. They agree with those obtained from Cr^{3+}:GSGG. The difference in the observed lifetimes in Cr^{3+}:GSGG and Cr^{3+}:YGG can be explained by the variation of mixing parameters. The temperature dependence of the lifetimes of the R_1-line and the broad band in Fig. 4 is represented by a two-level system. The data of R_1-line are fitted fairly well to a single curve calculated using (6) with $\tau_1=2.4\,ms$, $\tau_2=40\,\mu s$, and $\Delta E=450\,cm^{-1}$. The deviation of the data for the broad band from the calculated curve below 150 K may be due to the experimental precision because the intensity of the broad band is very weak at low temperatures.

Next, the other component of the broad band is considered. The lifetime (0.16 ms) being nearly equal to that (0.23 ms) of the broad band in GSGG must be due to Cr^{3+} ions for which the crystal field is even further reduced. The intensity ratio of the fast component (0.16 ms) to the slow component (2.5 ms) at 780 nm is twice as large as that at 760 nm. This fact indicates that the peak wavelength of the broad band with the lifetime (0.16 ms) is red-shifted compared to that with 2.5 ms. The energy level of the lowest excited state is reduced and the separation between ^2E and $^4T_2$ levels is even smaller than that of a Cr^{3+} ion in the stoichiometric composition, or of a Cr^{3+} ion with seven Ga^{3+} and one Y^{3+} nearest neighbour octahedral ions. Therefore, this component (0.16 ms) is likely to be due to Cr^{3+} ion in unit cells where two or more Ga^{3+} ions are replaced by Y^{3+}, or due to Cr^{3+} ions occupying dodecahedral sites where the crystal

field is much weaker than that at octahedral sites. The R_1-line from the Cr^{3+} ion may be fairly weak compared to that at 689.8 nm.

In conclusion, the lifetimes of the R-line and the broad band show variations in garnet crystals with different crystal fields. Trends in the luminescence decay time can be explained by the variation of mixing parameters between ^2E and $^4T_2$ produced by tunnelling.

Acknowledgements. One of authors (M.Y.) is indebted to SERC for a senior visiting fellowship in 1989 and the INAMORI foundation for financial support. The work at Strathclyde has been in general supported by SERC through research grants GR/D62670 and GR/D75557.

References

1. B. Henderson, G.F. Imbusch: Contemp. Phys. **29**, 235 (1988)
2. L.F. Deshazer, A. Pinto, L. Esterowitz (eds.): *Tunable Solid State Lasers II* (Springer, Berlin, Heidelberg 1986)
3. L.F. Mollenauer, J.C. White (eds.): *Tunable Lasers* (Springer, Berlin, Heidelberg 1988) Chap. 9
4. B. Struve, G. Huber: Appl. Phys. B **36**, 195 (1985)
5. B. Henderson, K.P. O'Donnell, A. Marshall, M. Yamaga, B. Cockayne: J. Phys. C **21**, 6187 (1988)
6. K.P. O'Donnell, A. Marshall, M. Yamaga, B. Henderson, B. Cockayne: J. Lumin. **42**, 365 (1989)
7. M. Yamaga, B. Henderson, K.P. O'Donnell: J. Phys. Condens. Matter **1**, 9175 (1989)
8. M. Yamaga, B. Henderson, K.P. O'Donnell, C.T. Cowan: Appl. Phys. B **50**, 425 (1990)
9. M. Yamaga, A. Marshall, K.P. O'Donnell, B. Henderson, Y. Miyazaki: J. Lumin. **39**, 335 (1988)
10. M. Yamaga, K. Yusa, Y. Miyazaki: Jpn. J. Appl. Phys. **25**, 194 (1986)
11. W.A. Wall, J.T. Kappick, B. Di Bartolo: J. Phys. C **4**, 3258 (1971)
12. J.C. Walling, O.G. Peterson, H.P. Jenssen, R.C. Morris, E.W. O'Nell: IEEE J. Quantum Electron. QE-**16**, 1302 (1980)
13. G.J. Quarles, A. Suchocki, R.C. Powell: Phys. Rev. **38**, 9996 (1988)
14. A. Suchocki, R.C. Powell: Chem. Phys. **128**, 59 (1988)
15. L.J. Andrews, S.M. Hitelman, M. Kokta, D. Gabbe: J. Chem. Phys. **84**, 5229 (1986)